AD-A124 571 RADAR DETECTION OF ICE WEDGES IN ALASKA(U) COLD REGIONS RESEARCH AND ENGINEERING LAB HANOVER NH S A ARCONE ET AL. DEC 82 CRREL-82-43 1/1

UNCLASSIFIED F/G 8/12 NL

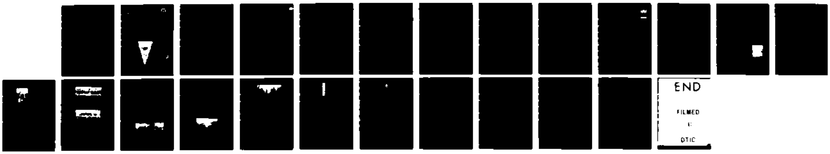

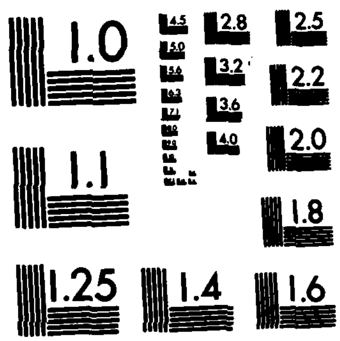

MICROCOPY RESOLUTION TEST CHART
NATIONAL BUREAU OF STANDARDS-1963-A

CRREL REPORT 82-43

US Army Corps of Engineers
Cold Regions Research & Engineering Laboratory

(12)

AD A 124571

Radar detection of ice wedges in Alaska

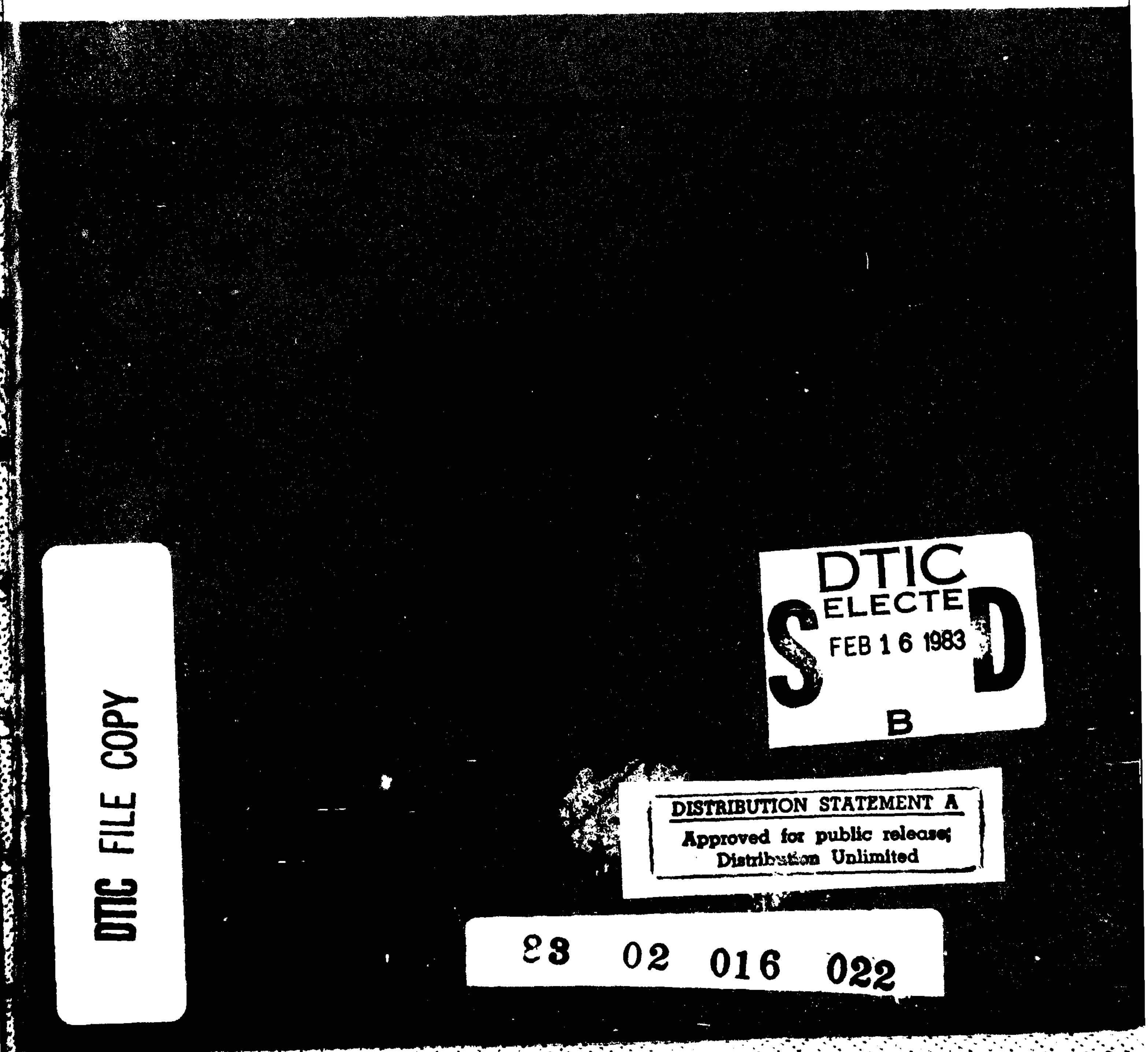

For conversion of SI metric units to U.S./ British customary units of measurement consult ASTM Standard E380, Metric Practice Guide, *published by the American Society for Testing and Materials, 1916 Race St., Philadelphia, Pa. 19103.*

Cover: Hypothetical refracted ray paths constructed to explain off-axis focusing seen in ice wedge radar returns.

CRREL Report 82-43

December 1982

Radar detection of ice wedges in Alaska

S.A. Arcone, P.V. Sellmann and A.J. Delaney

Prepared for
OFFICE OF THE CHIEF OF ENGINEERS
Approved for public release; distribution unlimited

Unclassified

SECURITY CLASSIFICATION OF THIS PAGE (When Data Entered)

REPORT DOCUMENTATION PAGE		READ INSTRUCTIONS BEFORE COMPLETING FORM
1. REPORT NUMBER CRREL Report 82-43	2. GOVT ACCESSION NO. AD-A124571	3. RECIPIENT'S CATALOG NUMBER
4. TITLE (and Subtitle) RADAR DETECTION OF ICE WEDGES IN ALASKA		5. TYPE OF REPORT & PERIOD COVERED 6. PERFORMING ORG. REPORT NUMBER
7. AUTHOR(s) S.A. Arcone, P.V. Sellmann and A.J. Delaney		8. CONTRACT OR GRANT NUMBER(s)
9. PERFORMING ORGANIZATION NAME AND ADDRESS U.S. Army Cold Regions Research and Engineering Laboratory Hanover, New Hampshire 03755		10. PROGRAM ELEMENT, PROJECT, TASK AREA & WORK UNIT NUMBERS DA Project 4A762730AT42, Task D, Work Unit 11
11. CONTROLLING OFFICE NAME AND ADDRESS Office of the Chief of Engineers Washington, D.C. 20314		12. REPORT DATE December 1982 13. NUMBER OF PAGES 19
14. MONITORING AGENCY NAME & ADDRESS(if different from Controlling Office)		15. SECURITY CLASS. (of this report) Unclassified 15a. DECLASSIFICATION/DOWNGRADING SCHEDULE

16. DISTRIBUTION STATEMENT (of this Report)

Approved for public release; distribution unlimited.

17. DISTRIBUTION STATEMENT (of the abstract entered in Block 20, if different from Report)

18. SUPPLEMENTARY NOTES

19. KEY WORDS (Continue on reverse side if necessary and identify by block number)

Alaska
Ice wedges
Land ice
Radar equipment

20. ABSTRACT (Continue on reverse side if necessary and identify by block number)

The radar signatures of ice wedges and wedge-like structures have been investigated for a variety of soil conditions. The radar used for this study emitted short sinusoidal pulses of about 10-ns duration with an approximate center frequency of 150 MHz. Most of the ice wedges existed at depths of about 1 m in a variety of silty and sandy soils with both frozen and thawed active layers. The position of the wedges was usually identified from corresponding surface features. An artificial ice wedge in coarse-grained alluvium was also profiled as well as wedge-like structures of fine silt in a coarse-grained glacial outwash. All wedges and wedge-like structures produced a hyperbolic reflection profile except when an active layer of thawed, saturated silt was present which eliminated returns from the wedges. The peaks of the hyperbolas were sometimes masked by reflections from the permafrost table or other material interfaces, and multiple

DD FORM 1473, 1 JAN 73 EDITION OF 1 NOV 65 IS OBSOLETE

Unclassified

SECURITY CLASSIFICATION OF THIS PAGE (When Data Entered)

20. Abstract (cont'd).

hyperbolas occurred at some sites. The dielectric constant of the host medium was often calculated from the linear portions of the hyperbolas and the results were verified by laboratory time domain reflectometry measurements performed on field samples. In some cases, hyperbolic profiles originated at several meters depth suggesting that deep ice wedges could be detected in areas of cold permafrost.

PREFACE

This report was prepared by Dr. Steven A. Arcone, Geophysicist, and Allan J. Delaney, Physical Science Technician, of the Snow and Ice Branch, Research Division, and Paul V. Sellmann, Geologist, of the Geotechnical Research Branch, Experimental Engineering Division, U.S. Army Cold Regions Research and Engineering Laboratory. Funding for this research was provided by DA Project 4A762730AT42, *Design, Construction and Operations Technology for Cold Regions*, Task D, *Cold Regions Base Support Design and Construction*, Work Unit 11, *Electromagnetic Geophysical Methods for Rapid Subsurface Exploration*, and also by the U.S. Geological Survey through the Office of the National Petroleum Reserve, Alaska (NPRA).

The authors wish to thank Donald Albert and Dr. K. G. Neave for technically reviewing the manuscript of this report, and especially Dr. Max Brewer for the support provided during their field studies in the NPRA.

The contents of this report are not to be used for advertising or promotional purposes. Citation of brand names does not constitute an official endorsement or approval of the use of such commercial products.

CONTENTS

ILLUSTRATIONS

RADAR DETECTION OF ICE WEDGES IN ALASKA

S.A. Arcone, P.V. Sellmann and A.J. Delaney

INTRODUCTION

Background

Geophysical exploration of permafrost is generally intended to define the boundaries of ice-bonded ground and to delineate zones rich in ground ice and massive ice. Massive ice features such as wedges and lenses are often of particular interest to the geotechnical engineer as their location can indicate regions where maximum thaw settlement may occur. To the geologist, the position, size and depth of the ice features can help to establish past climatic and depositional events. In this report we discuss the use of ground-probing radar to detect massive ice wedges.

Electrical and electromagnetic methods have been widely used for permafrost exploration because of the large contrasts in electrical properties which exist between thawed and frozen ground and, in some cases, between massive ice and ice-rich soil. Galvanic methods using arrays of electrodes have measured such contrasts in d.c. electrical resistivity to profile or sound geologic structure (e.g. Barnes 1965, Ogilvy 1967). These contrasts have also been exploited by magnetic induction (Hoekstra 1978, Arcone et al. 1979) and the radiowave methods of wave-tilt and surface impedance (Hoekstra et al. 1975, Arcone et al. 1979, Davis et al. 1976, Scott and Hunter 1977). The latter two methods have responded well to changes in near-surface resistivity, but they were often unable to provide similar detail on deeper structure because of their low frequency nature and because very few data points could be obtained at each survey station. Computer modeling has to be performed with these methods in order to determine geologic structure. Structures that are not composed of horizontal, homogeneous layers are extremely difficult to model.

In the 1970's, several researchers investigated the use of radar for permafrost exploration. Radar signals in the VHF band (50 to 150 MHz) penetrated well in some circumstances, revealed some interesting responses over areas of massive ground ice, and permitted more detail to be distinguished in some material than was possible with low frequency methods because of the short wavelengths involved. Bertram et al. (1972) first demonstrated that radar could be used to profile ice masses in permafrost. Their profiles from Barrow, Alaska, revealed responses to these features that are similar to our results. Unfortunately their report contains very little data analysis. Davis et al. (1976) and Annan and Davis (1976) showed good radar penetration in massive ice and measured the dielectric constant of ice-rich ground in the area of Tuktoyaktuk, Canada, by continually separating their radar antennas to obtain wide-angle reflection and refraction (WARR) soundings. Arcone and Delaney (1982) used this technique later over layered frozen ground containing disseminated ice. Kovacs and Morey (1979) performed radar profiles along a segment of the trans-Alaska pipeline haul road and compared two reflection horizons with the vertical distribution of massive ice along one profile over 305 m (1000 ft) in length.

The propagation and reflection of VHF ground radar signals are strongly influenced by the dielectric permittivity of different ground materials and the contrasts between them. Concurrently with the development of subsurface radar, the permittivity of many materials has been measured in the VHF-UHF bands by several researchers (e.g. Hoekstra and Delaney 1974, Wong et al. 1977, Topp et al. 1980). Most of this work has concentrated on soils. Hoekstra and Delaney (1974) and Delaney and Arcone (1982) have shown that at subfreezing temperatures the permittivity of soils exhibits a strong dependency on unfrozen water content, thus demonstrating that strong reflections can occur within permafrost at interfaces between different frozen soils or between frozen soils of different water contents.

Objectives and procedures

The objective of these studies was to investigate the response of subsurface radar to a specific massive ice feature, the ice wedge, considering variations in electrical properties of materials caused by seasonal change and material type. The presence of an ice wedge was usually indicated by polygonal ground patterns. It was not our intent to detect these wedges as their presence was already evident from surface features. Rather, our purpose was to show the character of ice wedge radar reflections on a continuous profile so that responses from inactive wedges, deep wedges, and smaller newly forming wedges without surface expression could be identified in the future. In some cases, deep wedges were discovered.

An artificial ice wedge buried in thawed, dry gravel was first investigated to determine the spatial nature of radar reflections from a feature with this geometry. Investigations were then carried out in Alaska over active ice wedges and wedge-like structures, the lateral dimensions of which could be fairly well documented from surface observations and logs of shallow drill holes. The investigations were carried out in both late summer and early spring. The soils containing the wedges were either predominantly silt or sand. The dielectric permittivities of these soils were determined both in the field from hyperbolic reflection profiles and in the laboratory using time domain reflectometry (TDR) on samples from the study sites.

EQUIPMENT USED

Radar

The radar system used was manufactured by GSSI* and has been extensively described elsewhere (Morey 1974, Davis et al. 1976, Annan and Davis 1976). We used their model 400 mainframe, model 700P control module and model 3105 transmitting and receiving antennas. The antennas, combined in one housing, are resistively loaded, bowtie dipoles separated approximately 30 cm. The transmitting antenna emits a pulse of several nanoseconds duration at a pulse repetition rate of about 50 kHz. The system samples the return signals to display an audio frequency facsimile. The time scale is determined from a supplied calibrator, the accuracy of which is estimated at ± 3%.

*Geophysical Survey Systems, Inc., Hudson, New Hampshire.

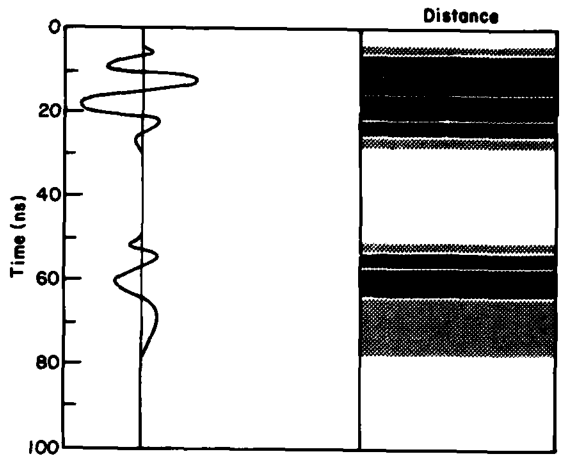

Figure 1. Hypothetical radar pulse returns and equivalent representation on the graphic record of these returns if unchanged along a short profile.

Profiling with the radar consists of towing the antennas over the ground surface and then displaying the echo returns graphically on electrochemically treated paper, or recording the signals on tape for future analysis. The graphic record is a consecutive series of A-scope (amplitude vs time) displays in which the horizontal axis is antenna position and the vertical axis is round-trip time of echo return. The signal amplitude is represented by the graphic intensity.

Figure 1 represents a radar return and how it would translate into the graphic record should that return be unchanged over a short profiling distance. The pulses oscillate longer than one period of the pulse center frequency so that several peaks are contained in one pulse or "event." Consequently, closely spaced returns may appear as one continuous oscillation on the graphic display.

The design center frequency of the 3105 antenna is about 300 MHz. Generally, the ground loads the antenna to reduce this to about 150 MHz. Increased gain was supplied to the later returns. The performance figure for this radar is estimated at between 60 and 70 dB.

TDR

The time domain reflectometry (TDR) method used for the laboratory studies has been described elsewhere (Loeb et al. 1971, Hoekstra and Delaney 1974) and will be reviewed. In TDR, step pulses are propagated along coaxial transmission lines and are reflected from soil or liquid samples contained at the end of the line. The TDR incident and reflected waveforms are Fourier-analyzed and compared with each other to derive the frequency-dependent reflection coefficient for the sample/air interface. The reflection coefficient is then converted to complex dielectric permittivity.

Generally, relaxation times for soil-water mixtures are less than 150 picoseconds (i.e. dispersions centered at 1 GHz or greater), so that the pulse reflections need only be monitored for about 800 ps to capture the entire reflection. The sample size was 20 cm long so that the round-trip distance for a reflection from the back of the sample was 40 cm. The fastest pulse propagation time possible in a sand or silt is about 20 cm/ns so that this sample length would delay a rear reflection by at least 2000 ps and thus not allow back-end reflections to interfere with the front-face reflection.

By 800 ps the waveform reflected from the sample has stabilized to a steady value, and we assume for data analysis that it would remain constant forever. This constancy is technically incorrect because a secondary relaxation due to d.c. conduction processes also occurs, but at a far greater relaxation time. Therefore these d.c. effects, which can be significant below 100 MHz, do not occur in our TDR data. They are also not important to our radar results because our radar bandwidth is mostly above 100 MHz.

The TDR pulse is a step waveform with a fast rise time of less than 35 ps. This assures sufficient energy in the 0.05 to 4-GHz range which easily covers our radar bandwidth. The fast rise times require that the time-dependent waveforms be reconstructed by sampling techniques. Sampling is performed by part of a Hewlett Packard 1815A system. The time-referencing procedures described by Loeb et al. and Samulon's modification of the Shannon theorem (Samulon 1951) were used in the waveform analysis. A thorough description of sample preparation is given in Delaney and Arcone (1982).

DEFINITIONS

Since we frequently refer to the electrical properties of materials in the ensuing discussion, a few definitions are in order. Under the assumption that electromagnetic waves propagate in proportion to $e^{i\omega t}$ (where t is time, ω is frequency in rad/s and $i = \sqrt{-1}$) the phase velocity v of any frequency component of a radar pulse that propagates in the ground is determined by the formula

$$v = \text{Real}\left\{c/\sqrt{\kappa^*(\omega)}\right\}. \tag{1}$$

The quantity c is the wave velocity in free space (30 cm/ns) and $\kappa^*(\omega)$ is the relative complex dielectric permittivity which is, in general, frequency dependent.

The quantity $\kappa^*(\omega)$ is further defined as

$$\kappa^*(\omega) = \kappa'(\omega) - i\kappa''(\omega) \tag{2}$$

where κ' is the real part and κ'' is the imaginary part. When $\kappa'' << \kappa'$, κ' is usually referred to as the dielectric constant (and it usually is constant with frequency under this restriction) and κ'' is usually referred to as the loss factor since it is directly proportional to wave attenuation in decibels. When κ' and κ'' are comparable, they are generally frequency dependent and cause wideband signals (pulses) to disperse or change shape due to the frequency components traveling at different speeds.

The frequency dependence of κ^* usually results from the presence of unfrozen water, either free or adsorbed. The dipolar nature of water causes dispersion generally between 100 MHz and 100 GHz with strongest effects occurring between about 2 and 30 GHz. The presence of ions in unfrozen water gives rise to an electrical conductivity σ (siemens/meter) which also contributes to κ^* through κ''. Therefore κ'' is usually composed of a conductive and dipolar contribution such that

$$\kappa'' = \frac{\sigma}{\omega\epsilon_0} + \kappa''_{\text{dipolar}} \tag{3}$$

where $\epsilon_0 = 8.85\times10^{-12}$ farad/meter. This conductivity factor is usually important at frequencies below 100 MHz as discussed above.

Materials such as ice, cold permafrost (<-5°C), dry soils, or granite can be ideal propagating media for radar because of their low (unfrozen) moisture content. In such cases $v = c/\sqrt{\kappa'}$. Where ice-rich permafrost is within a few degrees of 0°C, significant amounts of unfrozen water may be present in saline pore spaces or adsorbed on soil particle surfaces to cause significant wave dispersion or absorption.

When dispersion is not significant, the depth d of radar reflections is determined by using the formula

$$d = \frac{ct}{2\sqrt{\kappa'}}$$

This formula is applied to each layer in a layered medium and assumes that each layer is homogeneous.

Some references are given to WARR (wide angle reflection and refraction) soundings, which are seismic-type procedures during which the radar antennas are separated and individual traces are recorded for each separation. The method gives dielectric constants, and examples of its use in Alaska are given by Arcone and Delaney (1982).

MASSIVE ICE

Ground ice in permafrost occurs in several forms. It may occur as 1) small segregations or interstitially in voids between soil particles; 2) as large clear masses including larger ice segregations (lenses), pingo ice, and buried ice that originally formed on the surfaces; or 3) as ice wedges that grow in contraction cracks in frozen ground (Péwé 1975).

In this report we are concerned with the ice wedges that occur extensively throughout interior and northern Alaska. These wedges are commonly found in silts and fine sands, and occasionally occur in gravels in areas of cold permafrost. They are usually vertical. However, their shape can be extremely complex, depending on material type and stage of development. They may range up to 3 m in width and 10 m in height. Tops of buried wedges in the Fairbanks area have been documented to depths of 10 m (Sellmann 1967). Their distribution near the surface usually corresponds to an obvious polygonal relief pattern in areas where they are actively forming. Deeper, buried wedges, shallow inactive wedges, and smaller, newly forming wedges may not have a surface manifestation.

Wedge ice contains a very small quantity of fine sediment incorporated during wedge formation that gives the ice a foliated appearance. Air bubbles are also present. The dielectric constant κ' of pure ice at radar frequencies is 3.2; however, values as low as 2.6 (due to the presence of air) have been measured by Annan and Davis (1976) for ice-rich ground well below 0°C (see Davis [1979] for an explanation of of this). Therefore, values lower than 3.2 are also possible for massive ground ice. In contrast, ice-rich permafrost within 2 or 3 degrees of 0°C can have κ' values as high as 10.

RESULTS

Artificial wedge: Norwich, Vermont

Prior to our Alaska field studies, we investigated the response of our radar unit to a simulated ice wedge buried in a sand and gravel pit in Norwich, Vermont. The wedge was constructed of Styrofoam and enclosed in plastic. The dimensions of the wedge were approximately 1.5 m wide, 2.4 m long and 2.4 m deep. Its top was 1.0 m below the ground surface. The dielectric constant κ' of Styrofoam is approximately 1.1 and provides a dielectric contrast with dry sand and gravel ($\kappa' \simeq 4.0$) similar to that of wedge ice ($\kappa' \simeq 3.0$) with ice-rich silt ($6 < \kappa' < 10$) within a few degrees of 0°C.

The host material was a dry gravelly sand, the dielectric constant of which was measured at 7.0 using the WARR method. The sand and gravel backfill around and over the wedge was not as compact as the undisturbed material and probably was drier due to air exposure during excavation. Therefore, in the region of the wedge, we expected the dielectric constant of the sand and gravel to be lower than 7.0. The radar measurements discussed below gave a value of approximately 4.1.

Figure 2 shows a radar reflection profile across the width of the wedge. The geometric scale of the

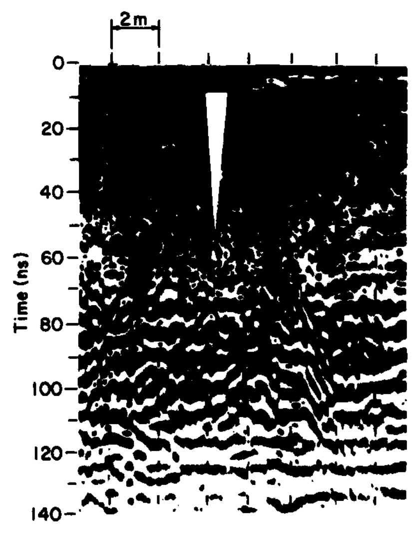

Figure 2. Radar profile over a Styrofoam wedge in sand and gravel. The location and scale of the wedge is shown by the white overlay whose vertical scale corresponds to a κ' = 7.

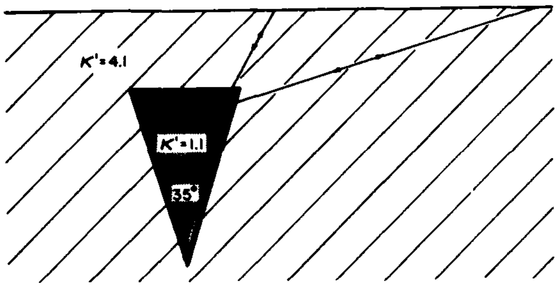

Figure 3. Hypothetical refracted ray paths to explain off-axis focusing seen in Figure 2. The in-situ wavelength of the pulse center frequency in the sand and gravel is comparable to the wedge dimensions so that diffraction theory would be needed to explain the total effect.

superimposed wedge corresponds to the time (assuming $\kappa' = 7.0$) and distance scales of the profile. The dark bands in the upper portion of the profile are caused by stratification in the sand and gravel, most likely due to drier conditions near the surface. The wedge appears to cause a broad hyperbolic return. Close inspection reveals this to be the superposition of three hyperbolas. A central hyperbola has its peak in the dark bands at a time delay of about 13 ns, which would correspond to a $\kappa' = 4.0$ for the wedge depth at 1 m. This central hyperbola is generated by the surface of the wedge and the linear portions of the hyperbola descend very obviously into the lighter portion of the record. The slope of these portions is approximately 13.6 cm/ns (cm of horizontal distance) which corresponds to a κ' value of 4.1.

The tops of the two other hyperbolas, whose linear portions quickly merge with those of the central one, can be seen near the lower portion of the wedge in Figure 2 at about 30 to 40 ns. The peaks of these two hyperbolas (the right one more obvious probably due to a slight incline in the vertical axis of the wedge) are displaced laterally from the edges of the wedge surface. Therefore, these secondary hyperbolas are probably caused by diffraction within the wedge, which is then focused off-axis as illustrated by some hypothetical ray paths shown in Figure 3.

The in-situ wavelength of the radar pulse center frequency in the wedge is about 1.5 m, which is the dimensional order of the wedge. Therefore diffraction theory rather than ray optics is needed to explain the total effect. In fact, the wedge may be acting as a resonant cavity and reemitting only in a narrow band of frequencies from within the entire radar band. This may explain the 6 or 7 bands seen on the hyperbola section between 90 and 110 ns.

Ice wedges in sand: Fish Creek, Alaska

This site was located a few miles west of the abandoned Fish Creek oil exploration site on the Arctic Coastal Plain. The site consists of a fine, inorganic eolian sand (Carter 1981). A laboratory analysis showed only 5% by weight of a sample of this sand to be silt size or smaller. The site was chosen because of its smooth surface and the presence of polygonal patterns associated with wedge ice.

Figure 4a shows a portion of a radar profile across ice wedges performed in mid-September 1980. The triangles above the horizontal axis indicate the center of troughs and, therefore, the approximate centers of the wedges. The dark bands between 15 and 20 ns are the reflections from the thawed active layer/frozen ground interface. The average depth of the active layer was about 70 cm, which, when coupled with the radar time delays, gave an average κ' value of 12.2 for the thawed sand. The slopes of the linear portions of the prominent central hyperbola are approximately 4 cm/ns which corresponds to a $\kappa' = 14.1$. Therefore, the top of the wedge must have been near the bottom of the active layer because this κ' value indicates that the edge diffraction was traveling through the active layer. This conclusion may seem to contradict the record of Figure 4a which appears to show the top of the hyperbola to occur about 15 ns after the first active layer bottom returns. However, the true peak of the hyperbola is masked by the dark bands of the active layer bottom reflection. The apparent peak is really a superposition of the hyperbolic bands and the other linear reflections.

Figure 4b gives a simplification of the active layer and ice wedge returns. The multiple hyperbolas are believed to be caused by multiple reflections in the active layer as illustrated in the figure, rather than from any effects within the wedge. This is because the (extrapolated) centers of the secondary hyperbolas seem to be coincident with the center of the wedge and their linear portions have the same slope as those of the primary.

Figure 5 shows a more extensive profile with the hyperbola discussed above just left of the center. A different print format caused this profile to differ in appearance from the record in Figure 4a. Several other hyperbolas are also recognizable. One is found below each trough mark, indicating the presence of the corresponding ice wedge. However, between 3 and 8 m and between 22 and 26 m, hyperbolas appear for which no surface indication was present. These may correspond with older, deeper ice wedges or small, newly forming wedges. Their relative age could be inferred by the position of the top of the hyperbolic reflections.

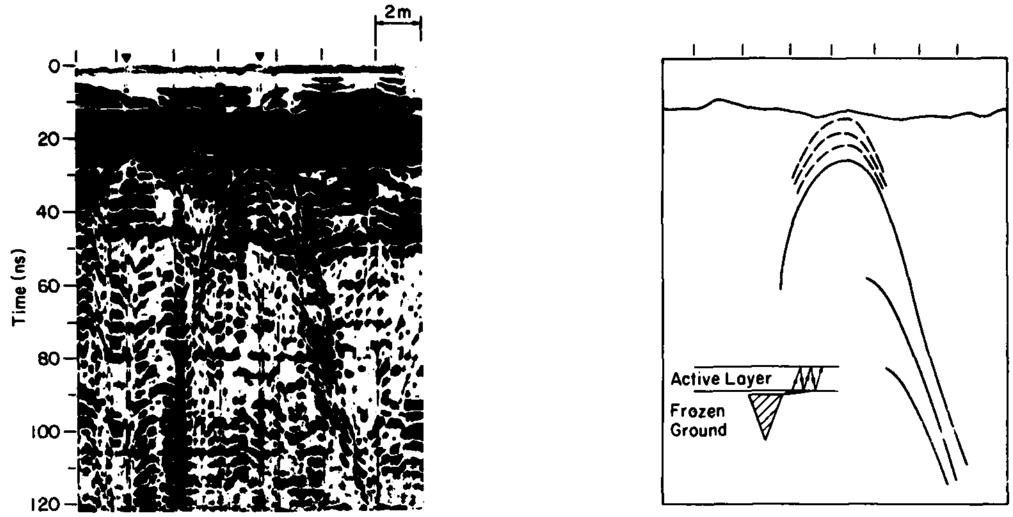

a. Radar profile. Triangles indicate position of surface troughs.

b. Some possible ray paths to explain the multiple hyperbolas.

Figure 4. Radar profile and simplification of significant returns for an ice wedge in sand near Fish Creek, Alaska.

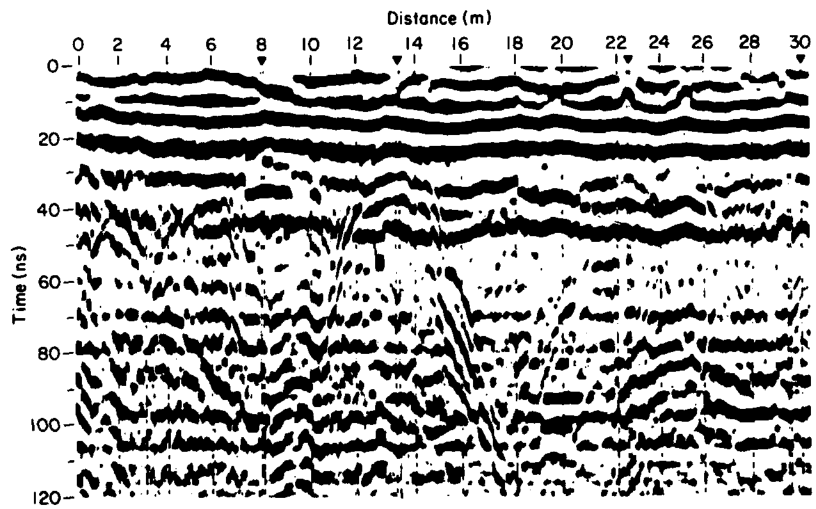

Figure 5. Radar profiles over a series of polygonal troughs near Fish Creek, Alaska. The hyperbola of Figure 4b is at a horizontal position of 13.5 m.

Ice wedges: Prudhoe Bay, Alaska

This investigation was carried out during late April of 1981. Radar profiles were performed over a polygonal ground area covered by 25 to 30 cm of snow. The surface soil was organic to sandy silt with the section becoming more coarse-grained below 2 to 3 m. The temperature of the sediments was probably below -10°C to at least a 3-m depth (Gold and Lachenbruch 1973). Attempts to measure the dielectric constant of the first few meters using a WARR sounding failed because antenna elevation due to snow cover strongly attenuates ground surface waves in the radar bandwidth. However, we estimate a value of 6.5 based on the hyperbola measurements discussed below.

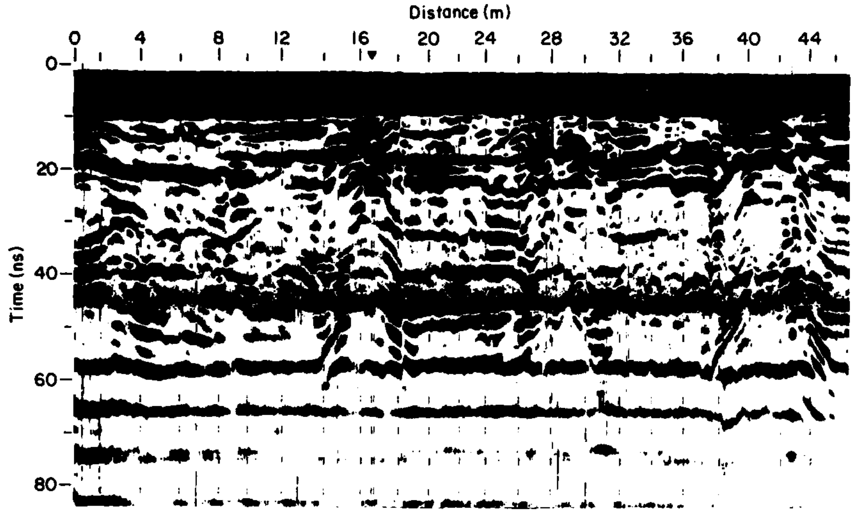

Figure 6. Radar profiles over ice wedges at Prudhoe Bay, Alaska. The hyperbolic peaks occur between 10 and 20 ns. Multiple reflections occur to over 65 ns.

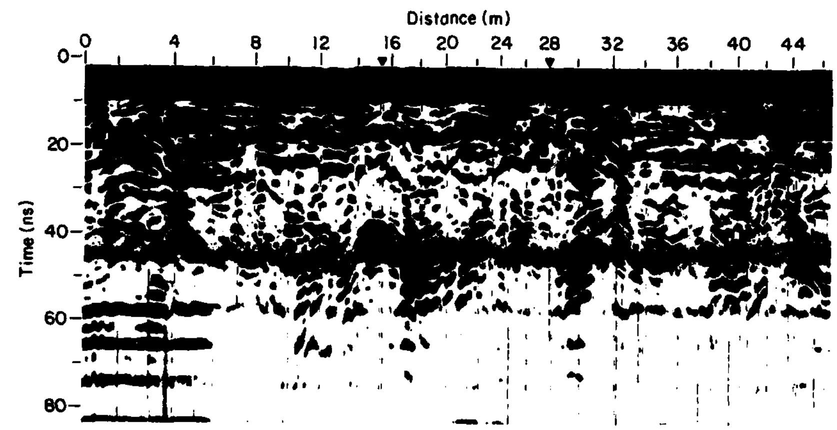

Figure 7. Radar profiles over ice wedges at Prudhoe Bay. The profile line is parallel to that of Figure 6.

Figures 6 and 7 show two radar profiles taken in parallel about 2 m apart. The triangles indicate the centers of polygon troughs observed along these lines. The numerous, irregular, thin vertical lines resulted from a minor system malfunction. The first dark horizontal bands at the top of the record commencing at 2 ns are returns from the snow/ground interface. Continuous, dark horizontal bands commencing at about 17 and 42 ns after the ground surface returns occur in both figures but most clearly on Figure 6. The return at 17 ns in Figure 6 cannot be from the active layer/permafrost interface (where a transition in ice content might occur) because this depth is about 40 cm, which gives a κ' value of over 30. However, the κ' value of 6.5, calculated from the linear portion of the hyperbola left of center in Figure 6, gives a depth of about 0.9 m for the 17-ns reflection. A κ' of 6.5 is a typical value for frozen silt (discussed below) so that this reflection may correspond to the fine-grained layer that caps this area or a change in ground ice content, but no borings were available or made to determine the actual nature of the reflector.

Several hyperbolas occur in both Figures 6 and 7 and each was correlated with a polygonal trough in the field. One of these troughs was further investigated with shallow drilling which confirmed the

the presence of wedge ice at approximately 1 m below the ground surface. This means that the peaks of the hyperbolas should come within 15 ns of the ground surface returns, as is evident in both figures, though these anomalous returns are distorted and somewhat masked by other returns. The prominent hyperbolic peak seen at about 40 ns in Figure 7 (at 15-m distance) is a multiple, the primary of which is masked by other strong returns between 10 and 20 ns.

Ice wedges under thawed fine grained soils: North Slope, Alaska

Two sites were profiled to determine whether ice wedges beneath a thawed, fine-grained active layer could be detected. Both sites were located on the Arctic Coastal Plain of Alaska and their surface soils were organic silts. The first study area was situated near an abandoned oil exploration site at East Oumalik in the National Petroleum Reserve, Alaska, approximately 170 km southwest of Lonely near the southern limit of the Arctic Coastal Plain. Degradation of the permafrost due to the exploration activities is now under study by CRREL and, as a result, some information is available on ground ice distribution. The sediments at this site consist of a thick section of ice-rich silt. The measured active layer thickness averaged 44 cm and the ground surface was extremely irregular due to polygonal troughs.

The profiles shown in Figure 8 were selected from a large amount of data obtained in mid-September 1980. Figure 8a shows a profile at East Oumalik that crossed two ice wedge troughs that were free of standing water. The intensity of the ground surface reflections were damped by the range gain settings. The heavy dark bands between 10 and 20 ns are primary reflections from the interface between the thawed active layer and the frozen sediments below. These reflections were used to calculate a mean dielectric constant of 32.7 for the thawed active layer at this site (Arcone 1982) which corresponds to an approximate volumetric water content of about 45% (Wang 1980). The radar returns beneath both marked troughs are complicated diffraction patterns and only a vague resemblance to a hyperbolic appearance can be seen beneath trough B when the record is viewed from an oblique angle. If these diffractions are hyperbolic, then the extended linear portions have been obliterated by the strong reflections from the permafrost table.

The second study area was situated near the runway at Lonely. A profile across two distinct troughs that contained no visible standing water is shown in Figure 8b. Between the indicated troughs a strong multiple occurs from about 25 to 40 ns. There is also a reflecting horizon at about 60 ns that does not seem to be a multiple, and therefore must be related to changes in material properties. This horizon fades beneath the marked troughs and no characteristic hyperbolic reflections are seen. This type of graphic display unfortunately does not permit signal intensity to be measured, or else it would be evident that the primary reflections beneath the troughs have less amplitude than in adjacent sections. This attenuation may be caused by higher moisture content of the lower trough areas and also possibly by a greater amount of diffuse scattering from the ice wedges.

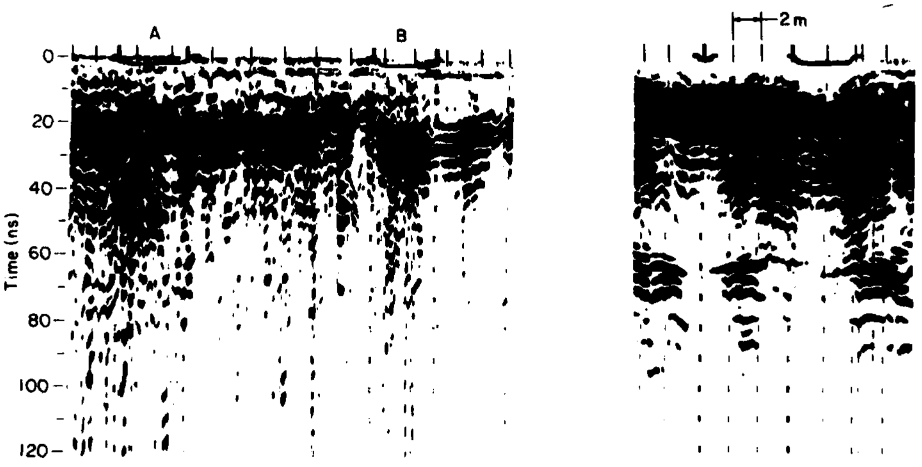

a. Two ice wedges in an ice-rich silt at East Oumalik.

b. Two ice wedges in an organic silt near the Lonely runway.

Figure 8. Radar profiles of ice wedges beneath a thawed active layer at two sites in the NPRA The symbols on the horizontal scale indicate position of polygonal troughs.

All profiles obtained over ice wedges in this area were similar with little penetration into the frozen sediments and no obvious hyperbolic reflections. Generally, the lack of such reflections can be explained by considering signal attenuation in a wet silt. At a center frequency of 150 MHz, the attenuation of a radar pulse in this type of medium for which the resistivity has been measured at 40 ohm-m (Arcone et al. 1978) is at least 15 dB/m. The loss due to reflection from the permafrost table is estimated at about 8 dB, transmission back through the surface loses another 5 dB, and geometric spreading of the beam may cause another 10 dB of loss. Therefore, for an active layer depth of about 0.5 m, between 35 and 40 dB of signal intensity is lost within the saturated troughs without even considering an initial loss due to inefficient antenna coupling with the ground and losses due to the finite size of any local diffractor such as an ice wedge. This loss is considerable when working with a radar system whose performance figure is only about 60 to 70 dB.

Wedge-like soil structures: Ft. Greely, Alaska

This site is a temporary runway surface over a glacial outwash plain near Donnelly Dome on the north flank of the Alaska Range. The outwash is stratified silt, sand and gravel. No permafrost exists here and there was no seasonal frost as our investigations were conducted in September 1980. The only modifications to the terrain were clearing of the organic cover and leveling of the surface. Numerous nearly vertical wedge-like soil structures exist to about 1.5-m depth and the structures of some of these features have been documented by Church et al. (1965). These structures join to form polygonal patterns at the surface similar to those associated with ice wedges. Sparse vegetation grows in the more fine-grained materials concentrated at the polygon margins, giving some indication of the distribution of these features. The horizontal beds adjacent to these wedge-like structures are generally distorted toward the vertical. WARR soundings made by Arcone and Delaney (1982) consistently give a value of $\kappa' = 5.5$ for the upper few meters of this site.

Figures 9 and 10 show two parallel radar profiles over a polygonal network of these wedge-like soil structures. Both profiles show two zones of radar returns. There are numerous events occurring earlier than about 50 ns that are characterized by closely spaced bands of continuous reflections. Hyperbolas with broad peaks originate at 20 ns or less under the horizontal bars that indicate surface expressions of the wedge-like structures. The slopes of the linear portions of the hyperbolas correspond with κ' values ranging between 3.5 and 9.4. For a κ' value of 5.5

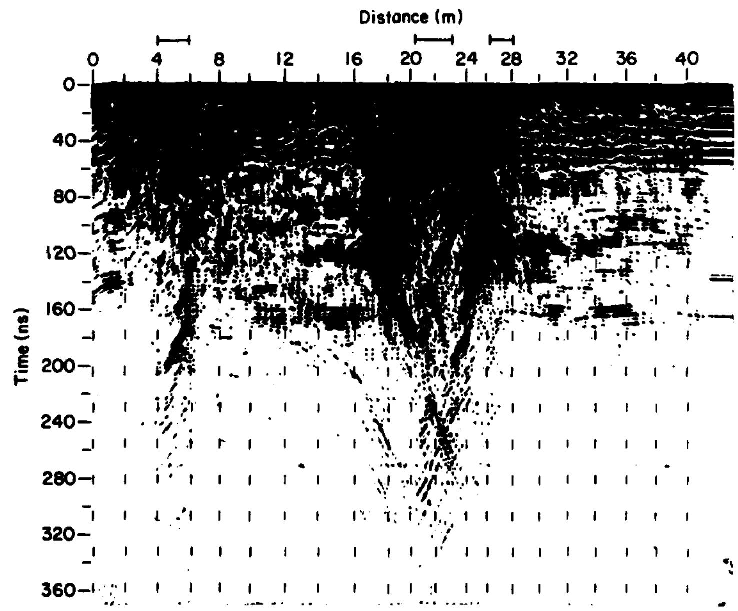

Figure 9. Radar profile over wedge-like structures at Ft. Greely, Alaska. Horizontal bars on the horizontal distance scale indicate the position of the structures.

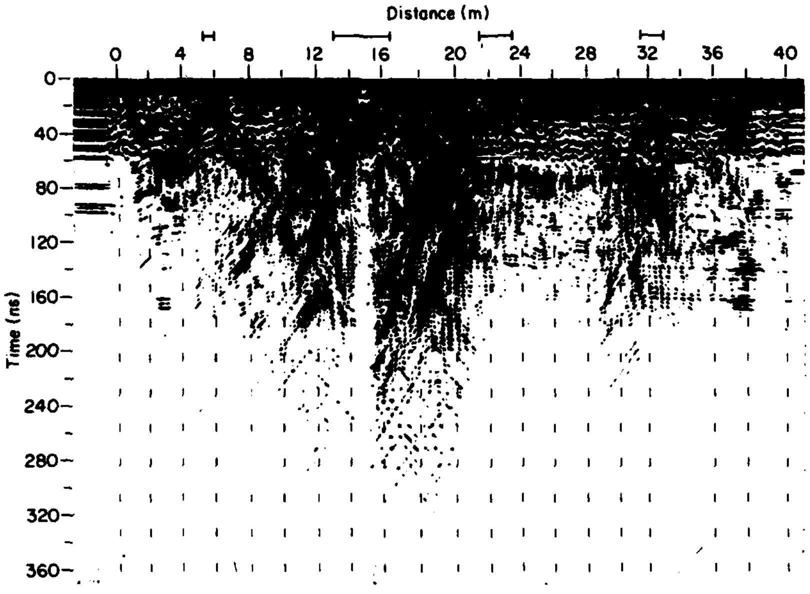

Figure 10. Radar profile over wedge-like structures along a line parallel to that of Figure 9.

(from WARR soundings) the peaks of these hyperbolas would occur within about 1.3 m of the surface and the 50-ns limit would correspond with a depth of 3.2 m, the maximum depth anticipated for the seasonal frost layer (Péwé and Holmes 1964). However, this 50-ns horizon may be a transition to more coarse-grained sediment.

In Figure 9, continuous bands corresponding to layering show up between 80 and 90, 120 and 130, and 160 and 170 ns at 12-to 16-m distance along the profile. In some places these returns are intersected by moderately dipping reflections giving a cross bedded appearance such as between 26 and 34 m at 80 to 120 ns. The numerous steeply dipping reflections are parts of hyperbolas with very narrow peaks and are believed to be edge diffractions from discrete inhomogeneities such as older wedge structures or horizontal changes in material type. Several dielectric constant values calculated from the linear portions of these diffractions ranged between 5.6 and 10.2.

TDR measurements

The dielectric permittivity of field samples of North Slope sand and Fairbanks loess were measured as a function of frequency to verify the dielectric contrasts observed in the field. The sand sample was from the active layer and had a gravimetric water content of 0.12 g water/g soil. The undisturbed volume of this sample was not known. However, the volumetric water content was about 25% when the original (undried) sample was packed in a coaxial sample holder. The silt sample was from the Fairbanks area but its dielectric properties may be compared with the results from the Oumalik site and the slightly coarser-grained surface soils at Prudhoe Bay. We assume that the water contents of the Oumalik and Prudhoe Bay soils were near saturation but no samples were obtained. However, the actual water content is relatively unimportant at very low temperatures, as will be seen below.

Figures 11-14 show the dielectric data acquired through TDR measurements. The pulse reflections were measured for 1000 ps to assure that the dipolar relaxations were monitored to completion; no secondary relaxations were observed within this time frame (as might be due to d.c. conduction). Therefore the d.c. conductivity for the soils studied (considering their moisture content and temperature) was believed to be sufficiently low so as to not significantly affect κ^* within or above the radar bandwidth.

Figures 11 and 12 show dielectric data for the North Slope sand. Figure 11 reveals that over the approximate radar bandwidth there is negligible dispersion, as κ' is constant both when thawed and frozen. The loss is extremely low at -3.1°C and still low at +7.6°C. The κ' value of 4.0 at -3.1°C does not vary much with decreasing temperature (as seen in Fig. 12) and only starts to rise significantly at about -2.0°C. The κ' value is also seen in Figure 12 to be independent of temperature, and the value

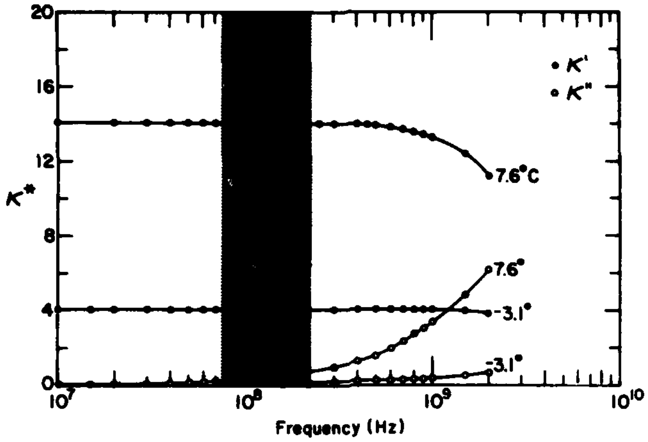

Figure 11. Complex components of the relative dielectric permittivity of North Slope sand as a function of frequency at two temperatures. The approximate 3-dB bandwidth of the radar pulse is shaded. The volumetric water content is 27%.

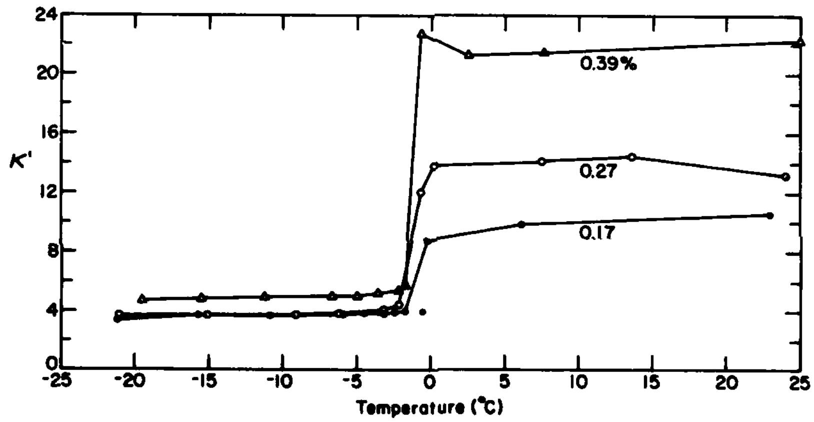

Figure 12. Real part of the relative dielectric permittivity of North Slope sand as a function of temperature for three volumetric water contents at the radar pulse center frequency of 150 MHz. The volumetric water content of the active layer sample from the site near Fish Creek was about 25%.

verifies the dielectric constant obtained from the hyperbolic returns seen in Figure 4a. The data points in Figure 12 apply only for 150 MHz and were taken from several TDR plots made at various temperatures.

Figures 13 and 14 show dielectric data for the silt. Figure 13 gives data for only one temperature, which is approximately that of the near-surface frozen ground at Prudhoe Bay for late April. The dielectric constant and loss are nearly independent of frequency over the radar band. The κ' value of 7.5 is close to the field measured value of 6.5 but the water content at Prudhoe Bay was unknown. However, the curves of Figure 14 show that the field measured value is reasonable for almost any water content below -2.0°C and that it is within the laboratory experimental error. Above freezing, the volumetric water content of 0.55 (corresponding to the κ' values of about 33 as was measured in the field; see Arcone 1982) verifies the observed saturated nature of the East Oumalik active layer.

The very slight dependencies upon initial water content seen in Figure 13 and to a lesser extent in Figure 12 are due to the fairly constant amount of adsorbed water that remains unfrozen as temperature falls below 0°C. At water contents above about 5-10%, all available soil surface area is taken up by

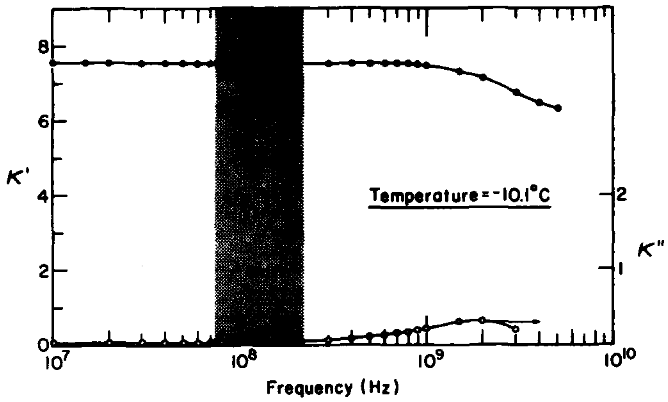

Figure 13. Complex components of the relative dielectric permittivity for an inorganic silt as a function of frequency. The approximate 3-dB bandwidth of the radar pulse is shaded. The volumetric water content is 36% and the temperature is -10.1°C.

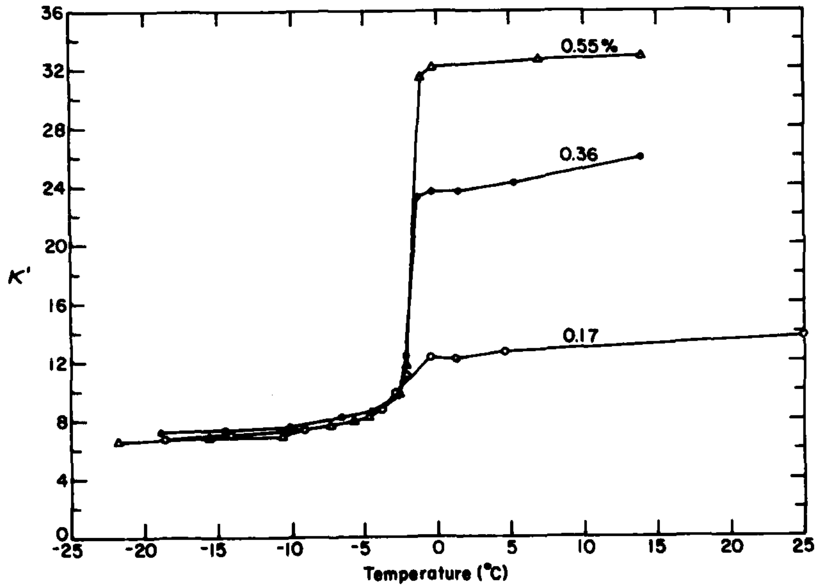

Figure 14. Real part of the relative dielectric permittivity for an inorganic silt as a function of temperature for three volumetric water contents at the radar pulse center frequency of 150 MHz. The ground temperature at Prudhoe Bay was approximately -12°C.

adsorbed water. Any more water added becomes free pore water, which freezes at temperatures just below 0°C. Since κ' for ice and dry silt is no greater than about 3.0, ice content will therefore no longer significantly affect the κ' of the ice-rich soil. In Figure 14, the slow decrease seen in κ' as temperature decreases well below freezing is caused by the slow freezing of adsorbed water.

SUMMARY AND CONCLUDING REMARKS

Ground radar responses to ice wedges in permafrost have been investigated. A Styrofoam wedge emplaced in a gravelly sand produced a radar response of several hyperbolic shapes when the profiling direction was across the width of the wedge. Real ice wedges in a frozen sand beneath a thawed active layer produced a simpler hyperbolic response containing a few multiples. Wedges in northern Alaska in cold, frozen, sandy silt beneath a frozen active layer gave the simplest hyperbolic profiles. Wedge-like soil structures and other unidentified inhomogeneities in outwash of sand and gravel produced a vast number of hyperbolic returns and multiples which were seen at the greatest time delay at all four sites. No significant response was obtained from wedges beneath a thawed, saturated active layer of organic silt. TDR measurements performed on soil samples verified the dielectric values measured in the field of the host media.

We conclude from these studies that ice wedges can be detected by radar operating at VHF in cold permafrost (colder than approximately -5°C) when the active layer is either frozen or well below saturation in a thawed state. VHF radar may penetrate a saturated active layer but too much energy may be lost during propagation in the active layer and from reflection from the permafrost. A dielectric contrast between the wedge ice and the host medium can usually be detected, but the ice and soil could be dielectrically identical under two circumstances. First, any absolutely dry soil would have a κ' value of about 3.0, but this is unlikely because soils containing ice wedges will contain ground ice. Secondly, values for ice and for clean, coarse-grained sediments with ice-filled voids can be very similar. However, most ice wedges occur in fine-grained materials.

Some of the hyperbolas seen in the field were similar to the main hyperbola seen over the artificial wedge, but the secondary hyperbolas observed in the Norwich study were never observed in the Alaskan studies. We do not know the exact depths of the Alaskan wedges but a higher frequency radar might give more detail because of its shorter wavelengths. As can be seen from Figures 11 and 13, pulse bandwidths between 500 and 1000 MHz would still not experience much loss or dispersion when propagating in frozen ground below about -5°C. Large losses would result in most thawed situations at UHF to microwave frequencies as can be seen in Figure 11.

The identification by radar of deep ice wedges or other local diffractors that were not associated with any surface expression was successful at two locations. At the Fish Creek site (Fig. 5) we assume that the unmarked hyperbolas are buried or newly forming wedges, and likewise at the Donnelly Dome site (Fig. 9 and 10) where a profusion of hyperbolas occurred beyond the 50-ns horizon. These returns demonstrate that radar profiling would be a useful method to detect, map and inventory buried ice wedges. It appears that surveys could be performed at depths up to 10 m in cold, nonsaline permafrost with the equipment we used, and probably over much greater depths with improved signal processing.

Future surveys using the seismic procedures of common depth-point signal stacking may be able to eliminate much of the unwanted coherent noise and reveal hyperbolic reflections that would ordinarily not be seen. Such surveys would require data to be recorded at discrete intervals rather than continuously as was done here. Although this procedure would consume more time per profile, a greater amount of information would be gained.

LITERATURE CITED

Annan, A.P. and J.L. Davis (1976) Impulse radar sounding in permafrost. *Radio Science*, vol. 11, no. 4, p. 383-394.

Arcone, S.A. (1982) Dielectric properties of the thawed active layer at VHF using radar. *Radio Science*, vol. 17, no. 3, p. 617-626.

Arcone, S.A. and A.J. Delaney (1982) Measurement of ground dielectric properties using wide-angle reflection and refraction. CRREL Report 82-6.

Arcone, S.A., A.J. Delaney and P.V. Sellmann (1979) Effects of seasonal changes and ground ice on electromagnetic surveys of permafrost. CRREL Report 79-23. ADA077903.

Barnes, D.F. (1965) Geophysical methods for delineating permafrost. *Permafrost: Proceedings of an International Conference*, Lafayette, Indiana, p. 349-355.

Bertram, C.L., K.J. Campbell and S.S. Sandler (1972) Locating large masses of ground ice with an impulse radar system. *Proceedings of the Eighth International Symposium on Remote Sensing of Environment*, Ann Arbor, Michigan, p. 241-260.

Carter, L.D. (1981) A Pleistocene sand sea on the Alaskan Arctic Coastal Plain. *Science*, vol. 211, p. 381-383.

Church, R.E., T.L. Péwé and M.J. Andersen (1965) Origin and environmental significance of large-scale patterned ground—Donnelly Dome area, Alaska. CRREL Research Report 159. ADXL474477.

Davis, J.L., W.J. Scott, R.M. Morey and A.P. Annan (1976) Impulse radar experiments on permafrost near Tuktoyaktuk, N.W.T. *Canadian Journal of Earth Sciences*, vol. 13, p. 1584-1590.

Davis, J.L. (1979) Electrical property measurements of sea ice in-situ using a wideband borehole radar and a time domain reflectometer. *Proceedings of the International Workshop on the Remote Estimation*

of Sea Ice Thickness, St. John's, Newfoundland, Memorial University, C-CORE Publication No. 80-5.
Delaney, A.J. and S. Arcone (1982) Laboratory measurements of soil dielectric properties between 0.1 and 5 GHz. CRREL Report 82-10.
Gold, L.W. and A.H. Lachenbruch (1973) Thermal conditions in permafrost—a review of North American literature. *Permafrost: Second International Conference*, North American Contribution, Yakutsk, USSR, National Academy of Sciences, Washington, D.C.
Hoekstra, P. and A. Delaney (1974) Dielectric properties of soils at UHF and microwave frequencies. *Journal of Geophysical Research*, vol. 79, no. 11, p. 1699–1708.
Hoekstra, P., P.V. Sellmann and A.J. Delaney (1975) Ground and airborne resistivity surveys of permafrost near Fairbanks, Alaska. *Geophysics*, vol. 40, no. 4, p. 641–656.
Hoekstra, P. (1978) Electromagnetic methods for mapping shallow permafrost. *Geophysics*, vol. 43, no. 4, p. 782-787.
Kovacs, A. and R.M. Morey (1979) Remote detection of massive ice in permafrost along the Alyeska pipeline and the pump station feeder gas pipeline. *Proceedings of the American Society of Civil Engineers Specialty Conference on Pipelines in Adverse Environments*, New Orleans, vol. 1, p. 268–280.
Loeb, H.W., G.M. Young, P.A. Quickenden and A. Suggett (1971) New methods for measurement of complex permittivity up to 13 GHz and their application to the study of dielectric relaxation of polar liquids including aqueous solutions. *Berichte der Bunsen-Gesellschaft fur Physikalische Chemie*, vol. 75, p. 1155.
Morey, R.M. (1974) Continuous subsurface profiling by impulse radar. *Proceedings of Engineering Foundation Conference on Subsurface Exploration for Underground Excavation and Heavy Construction*, New York: *American Society of Civil Engineers*, p. 213–232.
Ogilvy, A.A. (1967) Geophysical prospecting for groundwater in the Soviet Union. Geological Survey of Canada, Economic Geology Report 26, p. 641–650.
Péwé, T.L. (1975) Quaternary geology of Alaska. U.S. Geological Survey Professional Paper 835, U.S. Government Printing Office, Washington, D.C.
Péwé, T.L. and G.W. Holmes (1964) Geology of the Mt. Hayes D-4 Quadrangle, Alaska. USGS Miscellaneous Geologic Investigation Map I-394, U.S. Government Printing Office, Washington, D.C.
Samulon, H.A. (1951) Spectrum analysis of transient response curves. *Proceedings, Institute of Electrical and Electronics Engineers*, vol. 39, p. 175.
Sellmann, P.V. (1967) Geology of the USACRREL permafrost tunnel Fairbanks, Alaska. CRREL Technical Report *199. AD660310.*
Scott, W.J. and J.A. Hunter (1977) Applications of geophysical techniques in permafrost regions. *Canadian Journal of Earth Sciences*, vol. 14, no. 1, p. 117–127.
Topp, G.C., J.L. Davis and A.P. Annan (1980) Electromagnetic determination of soil water content: measurements in coaxial transmission lines, *Water Resources Research*, vol. 16, no. 3, p. 574–582.
Wang, J.R. (1980) The dielectric properties of soil-water mixtures at microwave frequencies. *Radio Science*, vol. 15, no. 5, p. 977–985.
Wong, J., J.R. Rossiter, G.R. Olhoeft and D.W. Strangway (1977) Permafrost: electrical properties of the active layer measured in situ. *Canadian Journal of Earth Sciences*, vol. 14, no. 4 (Part 1), p. 582-586.

APPENDIX A: BRIEF DISCUSSION OF DISPERSION

Dispersion occurs when the phase velocity and attenuation rate in a material or medium are frequency dependent over the bandwidth of a propagated pulse. In such cases, the pulse will lengthen with time, attenuate with propagation distance (above the usual $1/r^2$ energy attenuation rate in an unbounded medium) and various oscillations within the waveform will travel either forward or backward through the waveform as the pulse propagates. In a waveguide (e.g. two reflectors enclosing a lossless dielectric) phase velocity generally exceeds group velocity and attenuation increases sharply at some low frequency "cutoff." In this case, short pulses lengthen into a series of high frequency oscillations in a resonance effect. In an unbounded lossy material such as wet soil, above about 1 GHz κ^* is strongly frequency dependent. In this case, phase velocity is lower than group velocity, attenuation increases with frequency, and a short pulse will lengthen into a low frequency oscillation.

During the review of this report several issues were raised concerning the presence of dispersion in the data of this and other reports. These issues are italicized below and followed by one author's (S. Arcone's) discussion.

1. *Are resonance and waveguide dispersion present in Figures 2 and 4a, respectively, as evidenced by the disappearance with distance of phase fronts from the linear portions of the hyperbolas?*

In Figure 2, resonance would be caused by the dimensions of the Styrofoam wedge which would permit only higher frequencies to propagate. In Figure 4a, dispersion would be caused by the waveguide action of the active layer. This latter point is discussed in the text where dielectric property calculations show that propagation away from the wedge was taking place in the active layer.

2. *Does dispersion during propagation cause the center frequency of the radar pulses to decrease from about 300 MHz in air to about 150 MHz in ground?*

This effect is primarily due to antenna ground "loading" and occurs regardless of ground conductivity, although such frequency shifts are possible after a few meters of propagation through high conductivity ground. The loading is due to the induced radiation from the ground reacting on the antenna and thus slowing the velocity of current flow on the antenna. A resulting effect is to lower the resonant frequency of the antenna.

3. *Does the fact that radar echo bands are not all of the same width indicate that different frequencies are propagating at different velocities (e.g. a narrow band preceding a wider band would indicate that phase velocity was increasing with frequency) and thus that dispersion is present?*

This would be true if the pulse emitted from the antenna were initially composed of several bands of uniform duration. However, the basic pulse waveform is not uniformly oscillatory but is composed of several half cycles of various durations. This is a normal response to an antenna excitation current consisting of a Gaussian type of pulse.

4. *Were the TDR measurements performed in a sample cell that was too short and thus did not allow lower frequency material dispersions due to conductivity to reveal themselves because the skin depth generally exceeded the sample length?*

The length of a sample cell does not prevent a relaxation from occurring, but only from being allowed to go to completion without interference. When the sample cell is too short, rear end reflections interfere with the relaxation process. It is true that a sample cell must be greater than a skin depth (at all frequencies within most of the pulse's bandwidth) to accurately determine d.c. conductivity, but relaxations due to d.c. conductivity had hardly begun in our samples even after 1000 ps. Therefore we assume that conductivity values were low enough as to not affect the determination of dielectric properties over the radar bandwidth.

A fascimile catalog card in Library of Congress MARC format is reproduced below.

Arcone, S.A.
Radar detection of ice wedges in Alaska / by S.A. Arcone, P.V. Sellmann and A.J. Delaney. Hanover, N.H.: U.S. Army Cold Regions Research and Engineering Laboratory; Springfield, Va.: available from National Technical Information Service, 1982.
iv, 19 p., illus.; 28 cm. (CRREL Report 82-43.)
Prepared for Office of the Chief of Engineers by Corps of Engineers, U.S. Army Cold Regions Research and Engineering Laboratory under DA Project 4A762730 AT42.
Bibliography: p. 13.
1. Alaska. 2. Ice wedges. 3. Land ice. 4. Equipment. I. Sellmann, P.V. II. Delaney, A.J. III. United States. Army. Corps of Engineers. IV. Cold Regions Research and Engineering Laboratory, Hanover, N.H. V. Series: CRREL Report 82-43.

END